PHYSICAL REVIEW B VOLUME 17, NUMBER 8 15 APRIL 1978

Lattice dynamics of β-(silver iodide) by neutron scattering

W. Bührer* and R. M. Nicklow
Solid State Division, Oak Ridge National Laboratory, Oak Ridge, Tennessee 37830

P. Brüesch
Brown Boveri Research Centre, CH-5401 Baden, Switzerland
(Received 19 September 1977)

The dispersion relation for the normal modes of vibration in hexagonal β-AgI has been determined at 160 K along three principal symmetry directions from coherent neutron inelastic scattering data using a triple-axis spectrometer. The most interesting feature is the observation of a very-low-lying dispersionless TO mode which is almost decoupled from the other vibrations. The frequencies have been fitted by a valence-shell model, and a satisfactory agreement was obtained with four short-range parameters, a variable ionic charge, and mechanical and electrical polarizabilities for both ions. A frequency distribution function has been computed, together with the lattice heat capacity and the mean-square ionic displacement for each ion. The temperature dependence of the theoretical values compares well with the relevant experiments. Finally, the model is extended and the lattice vibrations of γ-AgI and α-AgI are discussed.

I. INTRODUCTION

Silver iodide has a number of crystallographic phases which have attracted attention for many years. At atmospheric conditions the hexagonal β modification (wurtzite) coexists with the cubic face-centered γ modification (sphalerite).[1] The connection to the other silver halides AgCl and AgBr occurs at 4 kbar, where AgI transforms to the rocksalt structure.[2] Due to the diffusion of silver ions through the lattice, β- and γ-AgI show already at room temperature a considerable ionic conductivity which, for example, is about eight orders of magnitude larger than that for NaCl.[3] At 147 °C there is a first-order phase transition to the famous high-temperature cubic α modification with statistically distributed silver ions[4,5] and a very high ionic conductivity, approaching that of liquid electrolytes.[6,7] α-AgI is the classical and most simple superionic conductor which has been studied extensively in the last few years.[8]

The migration of silver ions through AgI has found a wide technical application for a long time in the photographic process[9] and, more recently, in solid-state batteries where AgI and AgI-based compounds serve as solid electrolytes.[3,8,10] Because the diffusion of ions through crystals is a thermally activated process, the ionic conductivity is closely related to the phonon spectrum, and the knowledge of the lattice vibrations is therefore of prime importance for the understanding of the observed phenomena.

The structural and dynamical properties of the silver halides are governed by the competition of ionic bonding versus covalent bonding. The covalency is increasing from AgCl to AgBr and is strongest in AgI, giving rise to tetrahedral coordination. In the Phillips scale of ionicity,[11] AgI is the A^NB^{8-N} compound closest to the tetrahedral-octahedral phase transition. The octahedrally coordinated compounds have been extensively studied both theoretically and experimentally, including[12] AgCl and AgBr,[13-15] which are nearest to the above-mentioned transition on the octahedral basis. Lattice-dynamical models developed for ionic compounds[16] had to be extended to include covalent effects[17] in order to explain the observed dispersion curves in AgCl and AgBr. For AgI, on the other hand, a good model would probably be based on covalency, with addition of some ionic character. In particular, the parameters obtained from the lattice-dynamical calculations, such as the short-range force constants, the effective ionic charge, and the ionic polarizabilities enter directly into a microscopic calculation of the formation energy of Frenkel (or Schottky) defects.[18] In β-AgI the formation energy for defects is small compared with those of other simple diatomic salts (e.g., NaCl, NaBr, AgCl, and AgBr)[19] which is due to the weak interionic forces and the large polarizabilities of the Ag^+ and I^- ions in the wurtzite structure.

The phonon spectrum of β-AgI is also of importance for the ion dynamics of α-AgI: far-infrared studies have shown that the residual ray absorption observed in β-AgI survives the β-α phase transition and that the frequency of the TO mode in the α phase is approximately the same as in β-AgI.[20,21] This suggests, together with structural considerations,[22] that the forces are nearly the same in both phases. Therefore, the force constants of β-AgI will be useful zero-order parameters for the superionic conducting α-AgI.

In this paper we report neutron-inelastic-scattering measurements of the phonon dispersion

curves along the symmetry directions $\vec{\Sigma}$, $\vec{T}$, and $\vec{\Delta}$ in hexagonal β-AgI. Only a few wurtzite structured compounds[23,24] have been studied experimentally up to now and only modes in one symmetry plane have been observed. The details of our experiment and the resulting frequencies are given in Sec. II. The analysis of the data based on a valence-shell model[25] and the discussion of theoretical and experimental values of various physical properties of β-AgI is presented in Sec. III, together with an extension of the lattice-dynamical model to include γ-AgI and α-AgI. Some final conclusions are given in Sec. IV.

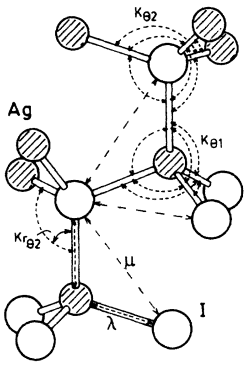

FIG. 1. Crystal structure of β-AgI (wurtzite) with internal force constants.

II. EXPERIMENT AND RESULTS

The structure of hexagonal β-AgI consists of stacked iodine tetrahedrons with a silver in the center (or vice versa) and is displayed in Fig. 1. There are two formula units in the primitive cell, giving rise to twelve phonon branches. β-AgI single crystals have been grown by slow diffusive dilution of a solution of AgI in concentrated aqueous KI solution.[26] The crystals were paleish yellow prisms (3.5 mm diameter, 25 mm long) with a [001] direction along the axis; the mosaic spread was better than 0.25°. The largest crystal was used for the measurement of the low-energy part of the dispersion curves; for the higher frequencies six crystals were mounted on a multigoniometer head where each crystal could independently be adjusted. Some physical constants of AgI are given in Table I.

Experiments were initiated at the Diorit reactor in Würenlingen.[22] Because of the high-absorption cross section of silver only limited information was obtainable. Therefore, the measurements were continued on a triple-axis spectrometer at the Oak Ridge High Flux Isotope reactor. The (002) plane of a Be crystal was used as monochromator, the analyzers were Be(002) and graphite(002) for high and low resolution, respectively. The analyzer energy was kept fixed, and only phonon creation processes were observed. Measurements of the dispersion curves were made for wave vectors along the symmetry directions $\vec{T}$, $\vec{T}'$, and $\vec{\Sigma}$ in the basal plane, and along the hexagonal axis $\vec{\Delta}$. The experiments were started at room temperature. The constant-$\vec{q}$ mode of operation was used for all except the LA branches, where constant-ω scans produced better results. Phonons were studied at locations in reciprocal space where the focusing conditions[27] and the inelastic structure factor,[28] calculated with a preliminary model,[22] were favorable. Strong anharmonic effects and the large Debye-Waller factor restricted the experiments to small $\vec{q}-\omega$ values; in addition, the eigenvectors and eigenvalues predicted by the simple model were only partially correct and useful. Experiments were continued at lower temperature. A mapping of the dispersion curves was performed at 160 K, and some phonons were also studied at 80 K. In order to observe and separate the differ-

TABLE I. Some physical constant of β-AgI, space group C_{6v}^4.

		80 K	295 K
Lattice constant [a]			
a (Å)		4.592	4.593
c (Å)		7.512	7.510
u		0.374	0.377
Optical-mode energies [b] (cm^{-1})	A_1(TO) and E_1(TO)	106	103
	A_1(LO) and E_1(LO)	124	
	$\Gamma_4(E_2)$	112	
	$\Gamma_4(E_2)$	17	
Transition temperature		147 °C	

[a] Reference 39.
[b] References 30–32.

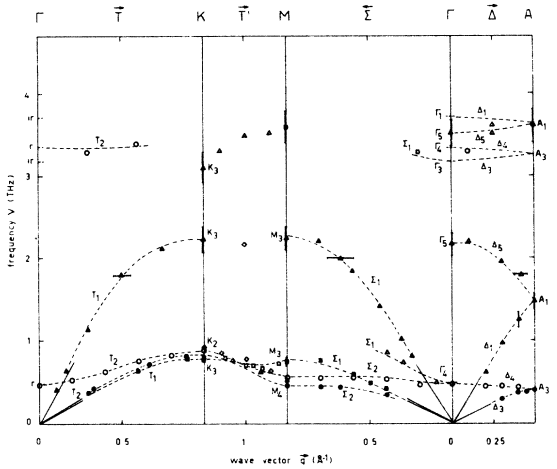

FIG. 2. Measured phonon dispersion curves of β-AgI at 160 K; polarization vectors (experimental): ▲ LA; ● TA perpendicular to $\vec{c}$; ■ TA parallel to $\vec{c}$; Δ LO; ○ TO perpendicular to $\vec{c}$; □ TO parallel to $\vec{c}$; ◇ unknown; ir-R, infrared-Raman (Refs. 30–32). The dashed lines are a guide to the eye; the solid lines are the velocities of sound (Ref. 33). The group-theoretical notation is according to Warren and Worlton (Ref. 29).

ent branches, the crystals had to be reoriented several times, that is with $(hk0)$, (hhl), $(h0l)$, $(3h+k, 2\bar{k}, h)$, and $(2h+k, 4\bar{h}, h)$ zones parallel to the scattering plane. The results at 160 K are shown in Fig. 2. The symbols give the dominant component of the polarization vector, as determined experimentally. The group-theoretical notation is according to Warren and Worlton,[29] and the dashed lines are a guide to the eye. The errors of the phonon frequencies due to the statistical uncertainty of the scattered neutron intensities are in the order of 0.03 THz for phonon energies smaller than 1 THz, and about 0.1 THz for the higher energies. Striking features of the dispersion relation of β-AgI are, compared to other wurtzite compounds,[23,24] the low energy of the TO mode in the zone center [symmetry $\Gamma_4(E_2)$] and the flat dispersion of all tne optic modes, resulting in two narrow energy bands for the upper six and the lower four modes.

Zone-center energies from infrared[30] and Raman[31,32] measurements agree within experimental errors with the present neutron data. Elastic constants of β-AgI have been determined by Fjeldly and Hanson,[33] the velocities of sound based on their data are shown in Fig. 2 (full lines through the origin), the agreement for the TA modes is very good.

The temperature dependence (300–80 K) of the lowest TO mode is very small, within experimental error, whereas the LA branches show a significant hardening by going to low temperature.

III. THEORETICAL CALCULATIONS AND DISCUSSION

A. Model analysis

In the wurtzite structure (space group C_{6v}^4), each Ag ion is tetrahedrally surrounded by four I ions and vice versa. Tetrahedral coordination is realized in the semiconductors of group-IV elements and extends with increasing Coulomb force contribution over III-V and II-VI to I-VII compounds. AgI is the $A^N B^{8-N}$ compound closest to the transition from tetrahedral to octrahedral coordination; its ionicity $f_{\mathrm{AgI}} = 0.77$ is just below the critical one, $f_c = 0.787$.[11]

Lattice vibrations of diatomic crystals with octahedral coordination (ionic bonding) have been successfully analyzed with the shell model.[16] An application to wurtzite,[34] however, showed that too many parameters were required for the description of the short-range forces. Tsuboi[35] introduced internal (valence) coordinates to determine the optically active zone center modes of sphalerite- and wurtzite-type crystals. This valence force potential concept was extended by McMurray *et al.*[36] to include all wave vectors and applied to group-IV elements. In a lattice-dynamical calculation of CdS, Nusimovici *et al.*[37] considered, in addition to these short-range forces, the effect of long-range Coulomb forces appropriate to vibrating polarizable ions with fixed charges and local vibration-induced displacements of the outer electrons relative to the core. A physically similar approach, the "valence-shell model" (VSM) has been used by Feldkamp *et al.*[25] for the analysis of cubic ZnS neutron scattering data. The VSM takes advantage of the short-range parameter economy of the valence force description for tetrahedrally coordinated systems, and combines it with the electrical and mechanical polarizabilities of the shell model.[16] The short-range part of the potential is expressed in terms of changes in bond distances, interbond angles and similar internal coordinates. In the present calculation for AgI, the stretching forces were restricted to first-neighbors silver-iodine and second-neighbors iodine-iodine interactions (the iodine forms an almost close packed lattice; the small silver ions are in the pockets in between). The short-range potential is given by

$$V^{SR} = \frac{\lambda}{2}\sum_{1-2}(\delta r_{ij})^2 + \frac{\mu}{2}\sum_{2-2}(\delta r_{ij})^2 + \frac{K_{\theta 1}}{2}r_0^2\sum_{2-1-2}(\delta\theta_{iij})^2 + \frac{K_{\theta 2}}{2}r_0^2\sum_{1-2-1}(\delta\theta_{ijk})^2 + \frac{Kr_{\theta 1}}{2}r_0\sum_{2-1-2}\delta\theta_{iij}\delta r_{ij} + \frac{Kr_{\theta 2}}{2}r_0\sum_{1-2-1}\delta\theta_{ijk}\delta r_{ij},$$

where r_0 is the nearest-neighbor distance and the indices 1 and 2 refer to silver and iodine; λ is the

first-neighbor and μ the second-neighbor stretching force constant; $K_{\theta 1}$ and $K_{\theta 2}$ are the angle-bending constants, and $Kr_{\theta 1}, Kr_{\theta 2}$ represent the stretching-bending interactions; δr_{ij} and $\delta\theta_{iij}$ are the respective changes in bond distances and bond angles (Fig. 1). In the long-range electrostatic part, the forces between the ions are assumed to act through the shells only. In view of the fact that β-AgI has an almost ideal wurtzite structure ($c/a = 1.636$, $u = 0.374$),[38,39] the polarizabilities of the ions were taken isotropically.

Values for the model parameters were obtained by a nonlinear least-squares procedure minimizing the χ^2 function

$$\chi^2 = \frac{1}{N-K} \sum_i \frac{(\nu^i_{\mathrm{obs}} - \nu^i_{\mathrm{calc}})^2}{(\delta\nu^i)^2},$$

where N and K are the number of phonons and parameters, respectively, and $\delta\nu^i$ is the experimental error of the ith phonon. Phonons with wave vectors corresponding to points Γ, M, and A were used in the fit, and the optical data were also included.

The first calculation was performed with a rigid-ion model. The result was not satisfactory; a serious disagreement between theory and experiment occurred for the lowest TO (LO) modes along $\vec{T}$ and $\vec{\Sigma}$; the computed curves showed a strong dispersion (Fig. 3, dotted lines) which was not observed experimentally. A much better agreement was obtained when the electrical and mechanical polarizabilities were introduced. During the computations, the stretch-bend interaction $Kr_{\theta 1}$ (silver in the center) turned out to be very small and was neglected for the subsequent calculations. The bending force constants $K_{\theta 1}$ and $K_{\theta 2}$ are set equal;

TABLE II. Valence-shell model parameters of β-AgI.

Stretch silver-iodine		$\lambda = 3.7 \times 10^4$ dyn/cm
Stretch iodine-iodine		$\mu = 4.5 \times 10^3$ dyn/cm
Bend-silver–bend-iodine		$K_{\theta 1} = K_{\theta 2} = -8.5 \times 10^2$ dyn/cm
Stretch-bend	Silver	$Kr_{\theta 1} = 0$
	Iodine	$Kr_{\theta 2} = -7.0 \times 10^2$ dyn/cm
Ionic charge		$z = 0.56e$
Polarizabilities	Silver	$\alpha_1 = 1.0$ Å^3
		$d_1 = 0.015e$
	iodine	$\alpha_2 = 3.0$ Å^3
		$d_2 = 0.050e$

a variation gave no definite improvement. The final model has nine parameters; four for the short-range part: silver-iodine and iodine-iodine stretching force constants, one bending constant and one stretch-bend interaction; and five long-range parameters: ionic charge, and the polarizabilities of Ag and I. The best set of parameters is given in Table II. The ionic charge is reduced to $0.56e$, and the electronic polarizabilities are considerably smaller than the free ion values.[40] The lines in Fig. 3 represent the calculated dispersion curves. The agreement with the experiment is good except for the LA modes which are calculated slightly too soft.

B. Derived properties of β-AgI

The phonon density of states $g(\nu)$ has been computed from the model with a program based on the method of Raubenheimer and Gilat.[41] The result is displayed in Fig. 4. The flat dispersion of the optic and the transverse acoustic modes gives rise to

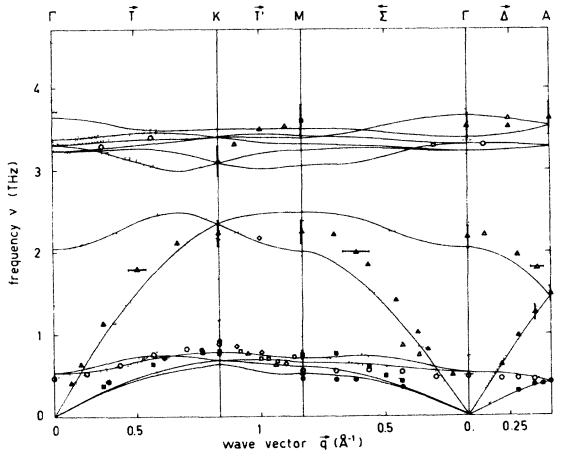

FIG. 3. Calculated phonon dispersion curves for β-AgI. Dotted lines: rigid-ion model; solid lines: valence-shell model.

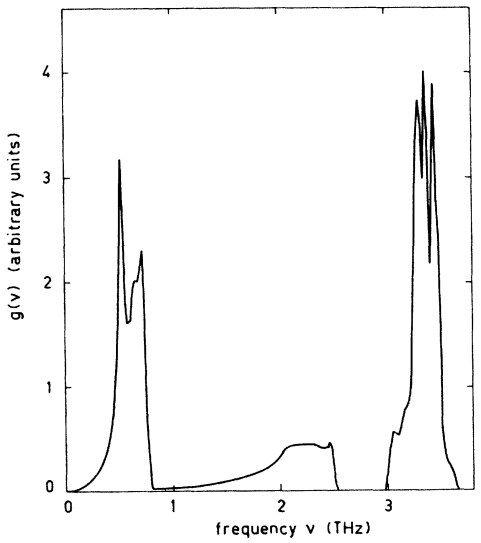

FIG. 4. Frequency distribution $g(\nu)$ for phonons, calculated with the VSM.

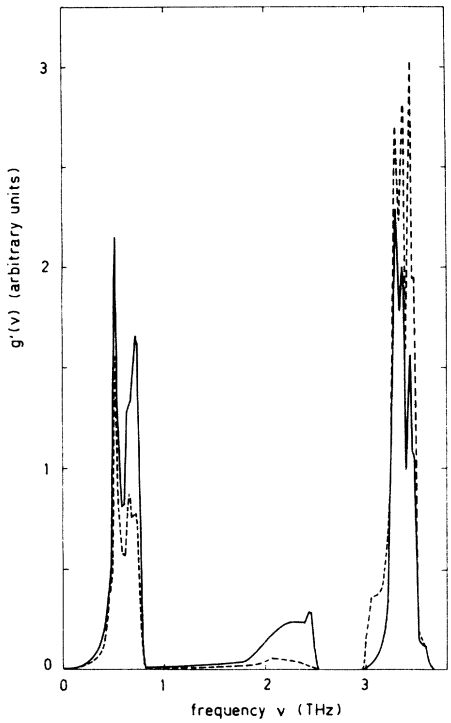

FIG. 5. Eigenvector weighted distribution functions $g'(\nu)$. Solid line: Ag^+ in β-AgI; dashed line: I^- in β-AgI.

two sharp maxima, separated by the broad distribution of the LA modes and a small frequency gap. In Fig. 5 the eigenvector-weighted density of states $g'(\nu)$ for Ag^+ and I^- in β-AgI are presented which have been calculated as described by Dolling *et al.*[42] Interesting is the clear separation of Ag and I eigenvectors in the LA and LO modes which contribute to both sides of the gap (2.3 and 3.1 THz, respectively).

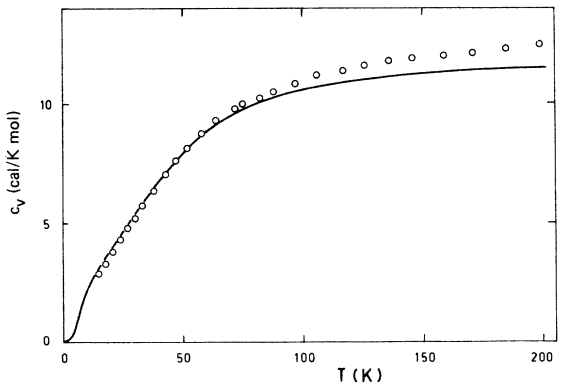

FIG. 6. Specific heat c_v(T) for β-AgI. Solid line: derived from Fig. 4 in the harmonic approximation; experimental points from Pitzer (Ref. 44).

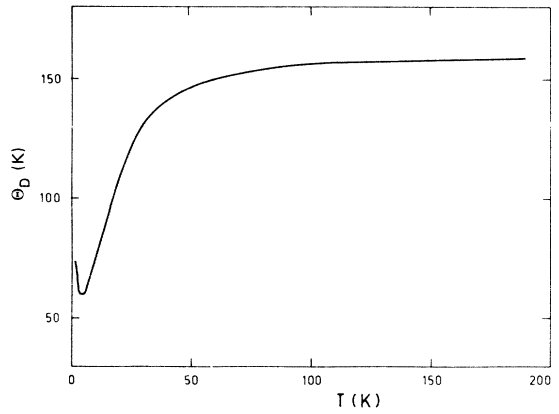

FIG. 7. Debye temperature $\Theta_D(T)$, as computed from the theoretical c_v values.

From the density of states $g(\nu)$ the specific heat has been calculated in the harmonic approximation[43] (see Fig. 6). Comparison is made with the experimental values of Pitzer.[44] Corrections $c_p \rightarrow c_v$ can be neglected for temperatures below 100 K because the volume expansion coefficient of β-AgI is very small. The linear behavior of the specific heat between 15 and 50 K is well reproduced by the calculation. This peculiar shape is a consequence of the "non-Debye" density of states $g(\nu)$, and does not depend on an asymmetric potential function of the silver ions.[44] At higher temperatures c_p has contributions from defect creation and anharmonicity and exceeds the computed c_v values. The calculated Debye temperature Θ_D (Fig. 7) shows a strong temperature dependence, in contradiction

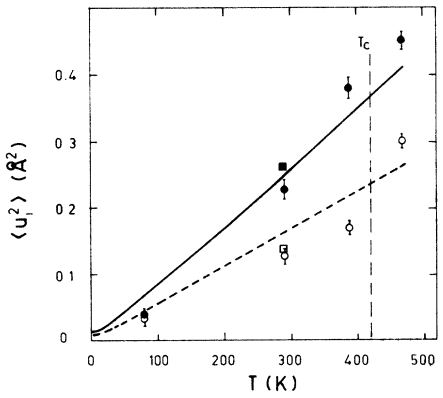

FIG. 8. Mean-square ionic displacements for Ag^+ and I^- in β-AgI, derived from Fig. 5. Solid line: Ag^+; dashed line: I^-; ●○ experimental points for Ag^+ and I^- from neutron scattering data (Ref. 47); ■ □ experimental points for Ag^+ and I^- from x-ray scattering data (Ref. 38).

TABLE III. Root-mean-square radial displacements at 295 K and melting points of silver halides.

		rms (Å)	T_s (°C)
Calculated	Ag in AgCl [a]	0.164	455
	Ag in AgBr [b]	0.173	434
	Ag in AgI	0.292	552
Experimental	Ag in AgI [c]	0.295 ± 0.008	
	Ag in AgI [d]	0.276 ± 0.011	

[a] Reference 12.
[b] Reference 14.
[c] Reference 38.
[d] Reference 39.

to a single-crystal, x-ray determination of Θ_D by Burley[45] who estimated a constant value ($\Theta_D = 119$ K) in the range 20–120 K.

The entropy at 298 K, calculated in the harmonic approximation[43] amounts to 27.8 cal/K mol, which is in excellent agreement with the experimental values of 27.6 ± 0.3 from heat capacity[44] and 27.6 cal/K mol from the temperature coefficients of the emf of a Ag-PbI_2 cell.[46]

By means of the weighted densities of states $g'(\nu)$, the mean-square ionic displacements for Ag^+ and I^- in AgI have been computed (Fig. 8). The theoretical curves compare well with the experimental points from x-ray[38] and elastic neutron scattering.[47] In Table III the rms radial displacements of silver at 295 K in the silver halides are listed. It is of interest to notice that Ag^+ in AgI has a much larger displacement than in AgBr or AgCl, although AgI has a considerably higher melting temperature than AgCl and AgBr.

C. γ-(silver iodide)

Tetrahedrally coordinated binary compounds of the $A^N B^{8-N}$ type are found in the cubic sphalerite or the hexagonal wurtzite structure. In AgI the two phases coexist at atmospheric pressure up to the transition to the α modification (147 °C). The γ phase is metastable over the entire range.[1] The difference between the two structures is another stacking sequence of planes of ions perpendicular to [001] in the hexagonal structure or to [111] in the cubic structure, resulting in a different arrangement of the basic tetraheders. Since β-AgI has an almost ideal wurtzite structure, it is easy to extend the present model to γ-AgI: the first neighbors are identical, and the second neighbors have the same distance, the difference appearing only in the long-range coulomb part. The calculated dispersion curve for γ-AgI, with no change in the model parameters, is shown in Fig. 9 for the high symmetry directions $\vec{\Delta}$, $\vec{\Sigma}$, and $\vec{\Lambda}$. Experi-

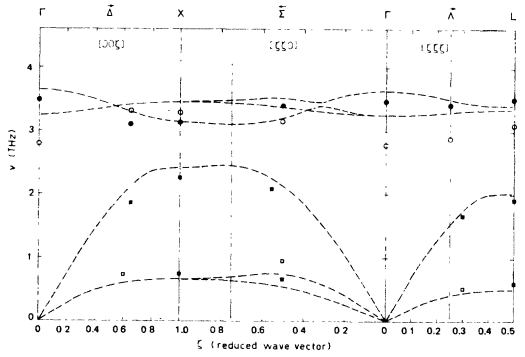

FIG. 9. Calculated phonon dispersion curves for γ-AgI (fcc), VSM model (dashed lines); the experimental points are CuBr values (Ref. 48), scaled by $(Ma^2_{CuBr}/Ma^2_{AgI})^{1/2}$.

mental phonon frequencies for γ-AgI do not exist because γ-AgI occurs only in powdered form. A compound with similar properties to AgI is CuBr, e.g., high ionic conductivity, phase transition to disordered phase, and ionicity $f = 0.73$. Experimental phonon frequencies of CuBr,[48] scaled by the homology criterion of interatomic forces

$$\omega_{AgI}/\omega_{CuBr} = (Ma^2_{CuBr}/Ma^2_{AgI})^{1/2},$$

where M is the mass number and a is the lattice constant of the compound, are given in Fig. 9. The agreement for room-temperature points is surprisingly good, indicating the relationship between AgI and CuBr and the applicability of the VSM model.

D. α-(silver iodide)

The superionic conducting α-AgI has a cubic body-centered structure. The highly mobile Ag^+ ions are statistically distributed on the 12 *d*) sites $(0, \frac{1}{4}, \frac{1}{2})$ of the space group O^9_h. The local structure and the interatomic distances in α-AgI are approximately the same as in β-AgI. Each Ag^+ ion of α-AgI is in the center of a distorted iodine tetrahedron, the nearest Ag-I distance is 2.833 Å, as compared to 2.808 Å $(0, 0, u)$ and 2.831 Å $(\frac{1}{3}, \frac{2}{3}, u - \frac{1}{2})$ in β-AgI. The distance between nearest iodine ions is 4.389 Å as compared to 4.593 Å in β-AgI. Spectroscopic experiments in the far infrared showed that the residual ray absorption near 3 THz survives the β-α transition and that the frequency of the TO mode is nearly the same in the two phases.[20,21] Both the structural and spectroscopic considerations suggest that the interatomic forces in α-AgI are similar to those of β-AgI. We have performed preliminary lattice-dynamical calculations of α-AgI using the force constants of β-AgI. In the model we considered a body-centered-tetragonal structure, space group D^9_{2d}, with iodine at

(0,0,0), silver at $(\frac{1}{2},0,\frac{1}{4})$, and $c_{tet}=a_{cub}$. This simple model neglects the effects of disorder and anharmonicity, but represents a structure with Ag^+ ions distributed uniformly and separated by relatively large distances of 4.389 Å. The calculated frequencies of the TO modes are near 3 THz, in good agreement with the experimental values. The lowest energies of the zone-boundary modes are about 0.5 THz and are further decreased if the electronic polarizabilities α_{Ag} and α_I are increased above the values given in Table II, or if the restoring forces for the silver ions are reduced as indicated by the low diffusion barrier for Ag^+ in α-AgI. The disorder in α-AgI will break the $\vec{q}$-selection rules as well as the symmetry of the unit cell, leading to a large number of optically active modes which might explain the weak low-frequency structure observed in the far-infrared and Raman spectra.

IV. CONCLUSIONS

Dispersion curves for the normal modes of vibration of β-AgI have been experimentally determined. The phonon spectrum is dominated by strong anharmonic effects, also observed in light-scattering experiments[31] and characteristic of all silver halides including[12] AgCl and AgBr.[13,14] Phonons with larger energy transfers such as LA phonons near the zone boundary or the high optic modes were heavily damped, even at 80 K, and measurements were extremely difficult. A further reduction of the sample temperature gave no definite improvement. The low-energy dispersionless TO modes $(\Delta_4, \Sigma_2, T_2)$, on the other hand, were easily observable, even at 295 K. They show no significant change of phonon energy or linewidth for temperatures between 80 and 295 K and behave as decoupled from the other lattice vibrations.

Besides the strong anharmonicity there are other reasons, specific to β-AgI, which prevented a complete mapping of all the twelve branches: (i) due to low symmetry along $\vec{\Sigma}$ and $\vec{T}$, the modes transform as only two different representations; thus the full benefit from selection rules[49] cannot be realized; (ii) the small energy separation of the optic modes, together with (i), leads to an interaction of the branches and; (iii) the scattered neutron intensity is further reduced due to the large Debye-Waller factor. Anharmonicity and the Debye-Waller factor could be reduced by going to very low temperature, which, however, in the present context is not desired because ionic conductivity and the phase transition occur at high temperature. We therefore concentrated our work to the six lower modes and the silent optic modes of symmetry Γ_5 (B_1). The experiments from the three symmetry directions give, together with the optical data, enough information for any lattice dynamical theory to be tested.

The central problem in a phonon dispersion calculation is the correct inclusion of a proper mixture of long- and short-range forces. β-AgI single crystals can easily be cleaved parallel to the hexagonal plane. The phonon spectrum, however, does not reveal the features of a layered compound, as, for instance, the structurally related graphite does. This indicates that the long-range isotropic electrostatic forces are important for β-AgI. The presently applied model includes both long- and short-range fields via a combination of valence forces and Coulomb forces. The shell model with four short-range and five long-range parameters provides a satisfactory fit to the observed dispersion relation. In the fitting procedure, the parameters did not take on unphysical values. The temperature dependence of experimentally determined thermodynamical properties like specific heat and mean-square ionic displacements can be well explained by the model, indicating the overall correctness of eigenvalues and eigenvectors. We are presently investigating whether the peculiar phonon dispersion of β-AgI gives rise to structured diffuse x-ray scattering.

The high ionic conductivity of β-AgI is due to Frenkel defects whose formation is closely related to the thermal motion of the ions. The flat low-energy modes give the major contribution to the thermal motion because they have a high density of states (Fig. 4) and are easily activated due to the low energy of 0.5 THz. Another important point is that it is mainly the silver ion which moves in the low energy modes (Fig. 5) although it is lighter than iodine. Moreover, the silver ion is much smaller than iodine, and therefore it will be favored for a jump to one of the many available interstitial positions of the wurtzite lattice. It should also be stressed that the low-frequency modes are mainly bond-bending modes in which only the tetrahedral angles are changed but not the Ag-I distances.[22] This leads to a very low value for the ratio of the bond-bending to bond-stretching force constant K_θ/λ, as can be seen from Table II. This is, however, not surprising since for $A^N B^{8-N}$ compounds with tetrahedral coordination a small value for the ratio K_θ/λ is expected if the ionicity of the AB bond $[f_i(\mathrm{AgI}) = 0.770]$ is close to Phillips' critical ionicity value $F_i = 0.785$.[11] The situation is drastically different for AgBr and AgCl. These compounds are more ionic $(f_i > F_i)$ and therefore crystallize in the NaCl structure which does not allow for low-frequency bending modes. Therefore, the mean-square amplitudes of vibration in AgBr and AgCl are much smaller than in β-AgI. At the β-α tran-

sition temperature of AgI ($T_c = 420$ K), the harmonic $\langle u^2 \rangle$ values of the silver ions of AgBr and AgCl are only about 30% of those of β-AgI and even at their melting temperatures (707 K for AgBr, 728 K for AgCl) these values are estimated to be only about 50% of the corresponding values of β-AgI at 420 K.[12,14]

No direct precursor effect to the β-α transition has been observed in the phonon spectrum; that is, there is no softening of any mode between 80 and 295 K, and the zone-center low-frequency mode of symmetry Γ_4 is stable up to the transition point.[32] The phase transition is driven by the entropy change ΔS due to the cation disordering, and the transition temperature is given by $T_c = \Delta H/\Delta S$, where ΔH is the change in the enthalpy. The detailed information we have gained about the elastic properties of AgI provides a starting point for the evaluation of $\Delta H = \Delta U + p\Delta V$. $p\Delta V$ is negligible; ΔU represents the difference in the total internal energies (short range plus long range) between the bcc structure of the α phase and the hexagonal structure of the β phase. The short-range contribution to ΔU can be estimated using the fact that the local structure and the interatomic distances in α-AgI are approximately the same as in β-AgI. Since the changes in the nearest Ag-I distances are very small and the bending force constants are negligible (Table II), a rough estimate shows that the main short-range contribution to ΔU originates from the change in the nearest I-I distances and involves the force constant μ in Table II. It would be interesting to compare the calculated value of ΔH with the observed value $\Delta H_{expt} = 1415$ cal/mol.[50] This involves not only the short-range contribution which accounts for about 50% of ΔH_{expt}, but also the contribution from the long-range electrostatic interactions. The latter contribution is difficult to evaluate; it represents the difference in the electrostatic energies between the disordered α phase and the ordered β-phase and depends on the ionic charges as well as on the ionic polarizabilities. Such a calculation is, however, beyond the scope of this paper.

ACKNOWLEDGMENTS

We would like to thank Mrs. A. Spiess from Brown Boveri for preparing the single crystals. We are grateful to Professor W. Hälg for his interest in this work, and to Dr. H. G. Smith from ORNL and Dr. H. U. Beyeler, Dr. L. Pietronero, Dr. S. Strässler, and Dr. H. R. Zeller from Brown Boveri for helpful discussions. This work was carried out during a visit of one of us (W.B.) at ORNL, and the hospitality extended by the Solid State Division is gratefully acknowledged.

*Permanent address: Institut für Reaktortechnik ETHZ, c/o E.I.R., CH-5303 Würenlingen, Switzerland.

[1] G. Burley, Am. Mineral. 48, 1266 (1963).
[2] W. A. Bassett and T. Takahashi, Am. Mineral. 50, 1576 (1965).
[3] H. Wiedersich and S. Geller, *The Chemistry of Extended Defects in Non-metallic Solids*, (North-Holland Amsterdam, 1970), p. 629.
[4] L. W. Strock, Z. Phys. Chem. B 25, 411 (1934); 31, 132 (1936).
[5] W. Bührer and W. Hälg, Helv. Phys. Acta 47, 27 (1974).
[6] C. Tubandt and E. Lorenz, Z. Phys. Chem. 87, 513 (1914).
[7] P. Junod, B. Kilchor and J. Wullschleger, Helv. Phys. Acta 44, 563 (1971).
[8] *Superionic Conductors: Chemistry, Physics and Applications*, edited by G. D. Mahan, (Plenum, New York, 1976).
[9] C. E. K. Mees and T. H. James, *The Theory of the Photographic Process*, (Macmillan, New York, 1966).
[10] *Fast Ion Transport in Solids, Solid State Batteries and Devices*, edited by W. van Gool (North-Holland, Amsterdam, 1973).
[11] J. C. Phillips, Rev. Mod. Phys. 42, 317 (1970).
[12] P. R. Vijayaraghavan, R. M. Nicklow, H. G. Smith, and M. K. Wilkinson, Phys. Rev. B 1, 4819 (1970).
[13] W. Bührer, Phys. Status Solidi B 68, 739 (1975).
[14] B. Dorner, W. von der Osten, and W. Bührer, J. Phys C 9, 723 (1976).
[15] Y. Fujii, S. Hoshino, S. Sakuragi, H. Kanzaki, J. W. Lynn, and G. Shirane, Phys. Rev. B 15, 358 (1977).
[16] A. D. B. Woods, W. Cochran, and B. N. Brockhouse, Phys. Rev. 119, 980 (1960).
[17] K. Fischer, H. Bilz, R. Haberkorn, and W. Weber, Phys. Status Solid (B) 54, 285 (1972).
[18] A. B. Lidiard, in *Encyclopedia of Physics*, edited by S. Flügge (Springer-Verlag, Berlin, Göttingen, Heidelberg, 1957), Vol. 20, p. 246.
[19] R. D. Armstrong, R. S. Bulmer, and T. Dickinson, J. Solid State Chem. 8, 219 (1973).
[20] P. Brüesch, S. Strässler, and H. R. Zeller, Phys. Status Solidi A 31, 217 (1975).
[21] P. Brüesch, L. Pietronero, and H. R. Zeller, J. Phys. C 9, 3977 (1976).
[22] W. Bührer and P. Brüesch, Solid State Commun. 16, 155 (1975).
[23] R. M. Brugger, K. A. Strong, and J. M. Carpenter, J. Phys. Chem. Solids 28, 249 (1967).
[24] K. Thoma, B. Dorner, G. Duesing, and W. Wegener, Solid State Commun. 15, 1111 (1974).
[25] L. A. Feldkamp, D. K. Steinman, N. Vagelatos, and J. S. King, J. Phys. Chem. Solids 32, 1573 (1971).
[26] G. Cochrane, Br. J. Appl. Phys. 18, 687 (1967).
[27] M. J. Cooper and R. Nathans, Acta Crystallogr. 23, 357 (1967).
[28] I. Waller and P. O. Fröman, Ark. Fys. 4, 183 (1952).
[29] J. L. Warren and T. G. Worlton, Argonne National Laboratory Report No. ANL-8035 (1973) (unpublished).
[30] A. Hadni, J. Claudel, and P. Strimer, Appl. Opt. 7, 1159 (1968).

[31]G. L. Bottger and V. C. Damsgard, J. Chem. Phys. 57, 1215 (1972).
[32]R. C. Hanson, T. A. Fjeldly, and H. D. Hochheimer, Phys. Status Solidi (B) 70, 567 (1975).
[33]T. A. Fjeldly and R. C. Hanson, Phys. Rev. B 10, 3569 (1974).
[34]J. J. Sullivan, J. Phys. Chem. Solids 25, 1039 (1964).
[35]M. Tsuboi, J. Chem. Phys. 40, 1326 (1964).
[36]H. L. McMurray, A. W. Solbrig, J. K. Boyter, and C. Noble, J. Phys. Chem. Solids 28, 2359 (1967).
[37]A. M. Nusimovici, M. Balkanski, and J. L. Birman, Phys. Rev. B 1, 595 (1970).
[38]G. Burley, J. Chem. Phys. 38, 2807 (1963).
[39]W. Bührer, Progress Report No. AF-SSP-68, Institut für Reaktortechnik ETHZ, CH-5303 Würenlingen, Switzerland, (1973) (unpublished).
[40]J. R. Tessman, A. H. Kahn, and W. Shockley, Phys. Rev. 92, 890 (1953).
[41]L. J. Raubenheimer and G. Gilat, Phys. Rev. 157, 586 (1967).
[42]G. Dolling, H. G. Smith, R. M. Nicklow, P. R. Vijayaraghavan, and M. K. Wilkinson, Phys. Rev. 168, 970 (1968).
[43]A. A. Maradudin, E. W. Montroll, H. G. Weiss, and I. P. Ipatova, Solid State Phys. Suppl. 3, 130 (1971).
[44]K. S. Pitzer, J. Am. Chem. Soc. 63, 516 (1941).
[45]G. Burley, J. Phys. Chem. Solids 25, 629 (1964).
[46]K. K. Kelley, US Bur. Mines Bull. 350, (1932); 394, (1936).
[47]W. Bührer, Progress Report No. AF-SSP-74, Institut für Reaktortechnik ETHZ, CH-5303 Würenlingen, Switzerland, (1974) (unpublished).
[48]S. Hoshino, Y. Fujii, J. Harada, and J. D. Axe, J. Phys. Soc. Jpn. 41, 965 (1976).
[49]R. J. Elliott and M. F. Thorpe, Proc. Phys. Soc. Lond. 91, 903 (1967).
[50]J. Nölting, Ber. Bunsenges. Phys. Chem. 67, 172 (1963).